# 西天山东塔尔别克金矿区安山岩 LA-ICP-MS 锆石 U-Pb 年代学、元素地球化学与岩石成因*

唐功建[1,2,3] 王强[1**] 赵振华[1] Derek A WYMAN[4] 陈海红[3] 贾小辉[1,2] 姜子琦[1,2]

TANG GongJian[1,2,3], WANG Qiang[1**], ZHAO ZhenHua[1], Derek A WYMAN[4], CHEN HaiHong[3], JIA XiaoHui[1,2] and JIANG ZiQi[1,2]

1. 中国科学院广州地球化学研究所同位素年代学与地球化学重点实验室,广州 510640
2. 中国科学院研究生院,北京 100039
3. 中国地质大学(武汉)地质过程与矿产资源国家重点实验室,武汉 4300474
4. 悉尼大学地球科学学院地质与地球物理系,新南威尔士 2006

1. *Key Laboratory of Isotope Geochronology and Geochemistry, Guangzhou Institute of Geochemistry, Chinese Academy of Sciences, Guangzhou* 510640, *China*
2. *Graduate University of Chinese Academy of Sciences, Beijing* 100049, *China*
3. *State Key Laboratory of Geological Processes and Mineral Resources, China University of Geosciences, Wuhan* 430074, *China*
4. *Division of Geology and Geophysics, School of Geosciences, The University of Sydney, NSW* 2006, *Australia*

2008-10-07 收稿,2008-11-18 改回.

**Tang GJ, Wang Q, Zhao ZH, Wyman DA, Chen HH, Jia XH and Jiang ZQ. 2009. LA-ICP-MS zircon U-Pb geochronology, element geochemistry and petrogenesis of the andesites in the eastern Taerbieke gold deposit of the western Tianshan region. *Acta Petrologica Sinica*, 25(6): 1341 – 1352**

**Abstract** The eastern Taerbieke gold deposit is geographically located to the south of the Axi gold deposit in the Tulasu basin, western Tianshan, and tectonically occurs in the western section of the Early Paleozoic Borohoro island arc between the Junggar plate to the north and the Yili-central Tianshan micro-plate to the south. The eastern Taerbieke andesites are geochemically similar to high-Mg andesite, e. g., high $SiO_2$ (58.94% ~63.85%) and MgO contents (3.75% ~6.59%), $Mg^{\#}$ values(58 ~69), and Cr ($94.2\times10^{-6}$ ~$241\times10^{-6}$) and Ni ($54.5\times10^{-6}$ ~$126\times10^{-6}$) contents, and low $FeO^{T}/MgO$ ratios. Except for slight low Sr contents ($235\times10^{-6}$ ~$696\times10^{-6}$), they are also geochemically similar to adakites, e. g., high $Al_2O_3$ (15.39% ~16.65 %), high Sr/Y(23.8 ~48.1) ratios, no significant Eu anomalies and clear depletion in Nb, Ta and Ti. LA-ICP-MS U-Pb age data suggest that the eastern Taerbieke andesites were generated in the Early Carboniferous (347.2 ± 1.6Ma). The enrichment in large ion lithophile elements (e. g. Rb, Th and U) and depletion in high field strength elements (e. g. Nb, Ta and Ti), and higher light rare earth element contents relative to heavy rare earth elements for the andesites, suggest that they are similar to island arc rocks. We suggest that the eastern Taerbieke andesites were possibly generated by the interaction between mantle and melts derived by partial melting of subducting sediments and altered oceanic crust during the subduction of Late Paleozoic northern Tianshan Ocean. The interaction between mantle and melts possibly played an important role in generating Au mineralization.

**Key words** Zircon LA-ICP-MS U-Pb dating; High-Mg addakite; Gold mineralization; Island setting; West Tianshan

**摘 要** 东塔尔别克金矿区位于西天山吐拉苏盆地内阿希金矿区南侧,构造上属于伊犁-中天山微板块与准噶尔板块之间的博罗科努早古生代岛弧带西段。东塔尔别克矿区出露有一些安山岩,这些岩石具有典型高镁安山岩特征,如高硅($SiO_2$ = 58.94% ~63.85%),具有较高的 MgO 含量(3.75% ~6.59%)和 $Mg^{\#}$(58 ~69)、高的 Cr($94.2\times10^{-6}$ ~$241\times10^{-6}$)、和 Ni

* 本文得到国家重点基础研究发展规划项目(2007CB411308)、中国科学院知识创新项目(KZCX1-YW-15-2, KZCX2-YW-128)和国家自然科学基金项目(40721063 和 40673037)的资助.

**第一作者简介**:唐功建,男,1979 年生,博士生,地球化学专业

** **通讯作者**:王强,男,1971 年生,博士,研究员,岩浆岩岩石学与地球化学专业,E-mail: wqiang@gig.ac.cn

($54.5\times10^{-6}$ ~ $126\times10^{-6}$)含量,以及低的 $FeO^T/MgO$ 比值。除了 Sr 含量略微偏低($235\times10^{-6}$ ~ $696\times10^{-6}$)之外,这些岩石基本显示了埃达克岩的地球化学特征:高的 $Al_2O_3$(15.39% ~16.65%),低 Y($9.86\times10^{-6}$ ~ $14.9\times10^{-6}$)含量,以及高的 Sr/Y 比值(23.8 ~48.1),无 Eu 异常,Nb、Ta、Ti 亏损等。LA-ICP-MS 锆石 U-Pb 测年结果显示安山岩的年龄为 347.2 ± 1.6Ma,为早石炭世。安山岩富集 Rb、Th、U 等大离子亲石元素,相对亏损 Nb、Ta、Ti 等高场强元素,轻重稀土元素分馏明显,具有俯冲带岛弧岩浆的特征。东塔尔别克安山岩可能形成于岛弧环境中,并可能由俯冲的晚古生代北天山洋洋壳以及少量上覆沉积物熔融形成,产生的熔体在上升过程中与地幔橄榄岩发生了相互作用. 熔体-地幔相互作用对区内金矿的形成具有重要意义。

**关键词** LA-ICP-MS 锆石 U-Pb 定年;高镁埃达克岩;金矿化;岛弧;西天山

**中图法分类号** P588.144;P597.3

## 1 引言

天山造山带是古亚洲洋造山带中的一个重要的造山带。一般认为天山造山带是在古生代由塔里木和西伯利亚板块之间的古亚洲洋的消减闭合,塔里木、准噶尔、哈萨克斯坦等板块的俯冲-碰撞-增生所形成(Coleman, 1989; Windley *et al.*, 1990; Allen et al., 1993; Sengör *et al.*, 1993; Shi *et al.*, 1994; Gao *et al.*, 1998; Xiao *et al.*, 2004; Liu and Fei, 2006)。其中在西天山的伊犁盆地的南北缘发育有大量的石炭纪岩浆岩(Xia *et al.*, 2004b, 2008; Zhu *et al.*, 2005; 王强等, 2006; 朱永峰等, 2006a,b; 朱志新等, 2006; 龙灵利等, 2008)。前人对西天山北部的石炭纪岩浆岩做了大量的工作,但目前对这些石炭纪岩浆岩的形成背景仍存在不同的认识,主要有大陆边缘岛弧(Gao *et al.*, 1998; Zhang *et al.*, 2003; Liu and Fei, 2006; Wang *et al.*, 2007b; Xiao *et al.*, 2008; Qian *et al.*, 2009; 王强等, 2006; 李锦轶等, 2006; 龙灵利等, 2008)还是裂谷(Xia *et al.*, 2004b, 2008; 车自成和刘良, 1996)或地幔柱环境(夏林圻等, 2004)之争。

天山造山带也是一个重要的 Cu-Au 等多金属成矿带,天山北缘出露有许多铜金矿床(点),如阿希、土屋、延东等。其中许多石炭纪岩浆岩与铜金成矿作用十分密切(Qin *et al.*, 2002; Rui *et al.*, 2002; Zhang *et al.*, 2006b, 2008; 王强等, 2006)。通过对岩浆岩的深入研究,有可能对深入了解金属矿床的成因、构造背景和地球动力学提供重要的启示。

本文首次对西天山北缘的阿希金矿区南侧的东塔尔别克金矿区的岩浆岩进行了 LA-ICP-MS 锆石 U-Pb 同位素年代学和元素地球化学研究,发现该区岩浆岩形成于早石炭世,并与阿希金矿的岩浆岩有类似的地球化学特征。本文将重点报道这一成果,并初步探讨其成因和形成的构造背景。

## 2 地质背景与岩相学

塔尔别克金矿位于科古琴山南坡断裂与伊犁盆地北缘断裂之间的吐拉苏盆地内(图 1b),南为伊犁 - 中天山板块,北为夹于伊犁-中天山板块与准噶尔板块之间的博罗科努早古生代岛弧带西段(图 1a)(Gao *et al.*, 1998)。塔吾尔别克金矿与阿希、京希、伊尔曼得、恰布坎卓它等金矿一起构成了

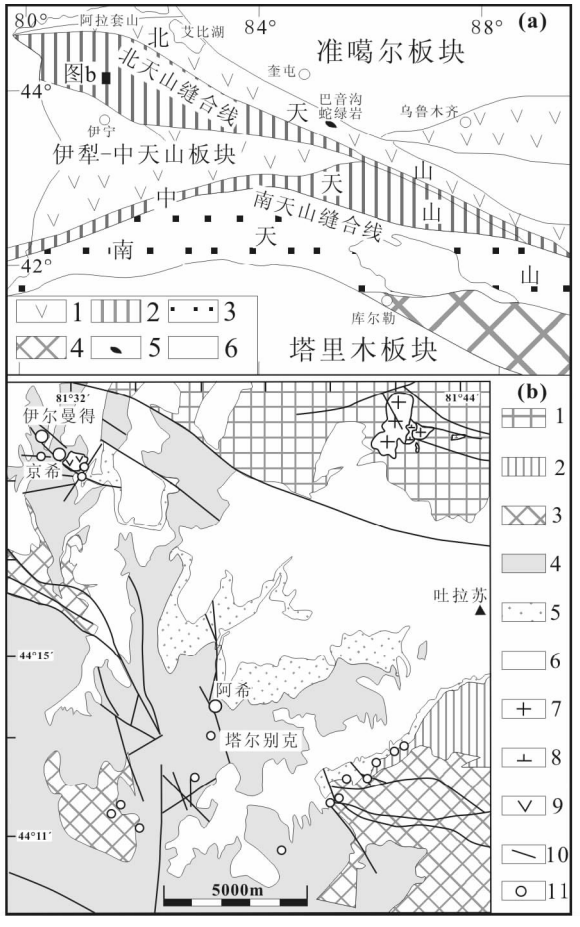


图 1 天山地区大地构造简图(a,据 Gao *et al.*, 1998 修改)和吐拉苏地区地质简图(b,据左学义等, 2005①)

(a): 1-晚古生代火山岩或火山碎屑岩;2-前寒武基底、古生代花岗岩和地层;3-古生代沉积岩;4-前寒武角闪岩相岩石;5-蛇绿岩;6-中新生带地层。(b): 1-前寒武纪;2-泥盆纪;3-早古生代;4-石炭纪大哈拉军组;5-石炭纪阿恰勒组;6-新生代沉积物;7-花岗岩;8-闪长岩;9-安山玢岩;10-断层;11-矿床或矿点

Fig. 1 Simplified geological map of the western Tianshan (a, after Gao *et al.*, 1998) and regional geological sketch map of the Tulasu areas (b)

① 左学义, 漆树基,伊发源. 2005. 吐拉苏金矿带大型金矿床定位预测. 新疆优势矿产资源勘查评价研究(305 项目, 2003BA12A-06-10)

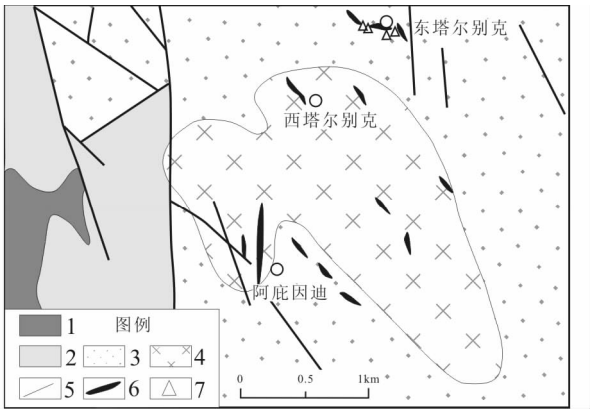


图 2　塔尔别克金矿矿区地质简图(据贾斌等,2001 修改)

1-奥陶系奈楞格勒达板组;2-大哈拉军山组第 1,2 和 4 岩性段;3-大哈拉军山组第 5 岩性段;4-二长斑岩;5-断层;6-金矿体;7-采样点

Fig. 2　Geological sketch map of the Taerbieke gold deposit (after Jia *et al.*, 2001)

吐拉苏金矿带。该区石炭纪岩浆岩分布广泛,并主要以石炭纪火山岩为主(Zhu *et al.*, 2005; 王强等, 2006; 朱志新等, 2006; 李华芹等, 2006; 龙灵利等, 2008)。该区出露的石炭纪火山岩属于大哈拉军山组。西天山地区的大哈拉军山组火山岩主要由玄武安山岩、安山岩、粗面安山岩、粗面岩、凝灰岩和英安岩组成(Zhu *et al.*, 2005; 朱永峰等,2005;左学义等, 2005; 龙灵利等, 2008),其形成时代为 354 ~ 312Ma (Zhu *et al.*, 2005)。

塔尔别克金矿区包括东西两个部分(图 2)。西塔尔别克金矿区以二长花岗斑岩为主,东塔尔别克金矿区以火山岩为主,后者也是本文研究的重点。东塔尔别克金矿区的西侧出露大哈拉军组第 1、2 和 4 岩性段火山岩,它们与奥陶系奈楞格勒达板组不整合接触。矿区广泛出露的地层为大哈拉军组第 5 岩性段火山岩,岩性主要由辉石安山岩、英安岩和凝灰岩组成。其中新鲜安山岩为紫红色,斑状结构,斑晶约占 5% ~10%, 以斜长石为主,同时含有少量的角闪石和普通辉石,其中斜长石呈自形板状的居多,最大可达 3mm,斜长石和辉石为半自形,基质以斜长石为主,斜长石有些短柱状,有些呈针状,具有玻晶交织结构,还有少量辉石和 Fe-Ti 氧化物。而蚀变的安山岩为土黄色,也为斑状结构,斑晶以斜长石为主,并大多已经绢云母化,还含有角闪石和石英,其中有些角闪石出现暗化边,有些蚀变为绿泥石或黑云母,基质为微细粒的绢云母化斜长石和钾长石、石英、角闪石和黑云母等,角闪石和黑云母均也都出现暗化边,另外,岩石中有些碳酸盐矿物充填。

## 3　分析方法

主、微量元素的分析测试均在中国科学院广州地球化学研究所同位素年代学和地球化学重点实验室完成。主量元素分析是用 Rigaku RIX 2000 型荧光光谱仪(XRF)分析,其详细步骤与 Li *et al.* (2005)所述相同。样品的含量由 36 种涵盖硅酸盐样品范围的参考标准物质双变量拟合的工作曲线确定,基体校正根据经验的 Traill-Lachance 程序进行,分析精度优于 1% ~5%。微量元素的分析则采用 Perkin-Elmer Sciex ELAN 6000 型电感耦合等离子体质谱仪(ICP-MS),具体的流程见 Li (1997)。使用 USGS 标准 W-2 和 G-2 及国内标准 GSR-1、GSR-2 和 GSR-3 来校正所测样品的元素含量,分析精度一般为 2% ~5%。分析数据列于表 1。

为精选锆石样品,先将新鲜的岩石样品粉碎至 120 目以下,用常规的人工淘洗和电磁选方法富集锆石,再在双目镜下用手工方法逐个精选锆石颗粒,未用任何化学试剂。本次锆石定年样品和主元素和微量元素分析的样品相对应。锆石阴极发光图像研究在中国科学院广州地球化学研究所 JXA-8100 电子探针仪上完成。锆石 LA-ICP-MS U-Pb 年龄测定在中国地质大学(武汉)地质过程与矿产资源国家重点实验室完成。ICP-MS 为 Agilent 公司生产的四极杆 ICP-MS Agilent 7500a,激光剥蚀系统为德国 Lamda Physik 公司的 GeoLas 2005 深紫外(DUV) 193 nm ArF 准分子(excimer)激光剥蚀系统。实验中采用 He 作为剥蚀物质的载气, 激光斑束直径为 32μm。参考物质为美国国家标准技术协会研制的人工合成硅酸盐玻璃 NIST SRM610,锆石 U-Pb 年龄的测定采用国际标准锆石 91500 作为外标进行校正, 每隔 5 个分析点测一次标准,保证标准和样品的仪器条件一致。在样品分析前后以及每隔 20 个测点各测一次 NIST SRM610, 以 Si 做内标,测定锆石中的 U, Th, Pb 的含量。详细的分析流程及有关参数见(Yuan *et al.*, 2004; Liu YS *et al.*, 2008)。元素的比率和元素的含量用 GLITTER(4.0 版)来处理,年龄的计算和谐和图用 ISOPLOT(3.00 版)(Ludwig, 2003)来完成。分析数据列于表 2。

## 4　分析结果

### 4.1　LA-ICPMS 锆石 U-Pb 定年

东塔吾尔别克安山岩样品 06XJ-31 的锆石多呈棱柱状,长约 40 ~ 120μm,长宽比在 1∶1.5 ~ 3∶1。阴极发光图像显示发育有清晰的韵律结构(图 3),锆石具有比较均一的 U/Th 比(1.27 ~ 3.30),大部分在 1.5 ~ 2.0 之间,为典型的岩浆锆石(U/Th > 1)。25 个分析点中有 23 个 $^{206}Pb/^{238}U$ 表面年龄在 340 ~ 351Ma 之间,在误差范围内比较一致,其加权平均值为 347.2 ± 1.6Ma(MSWD = 0.68)(图 3)。分析点 9 落在谐和线上,其 $^{206}Pb/^{238}U$ 表面年龄为 447 ± 6Ma,该锆石成板柱状,无岩浆环带(图 3),可能为奥陶纪火山岩的捕获晶。另有一个分析点(点 6)也靠近谐和线,其 $^{206}Pb/^{238}U$ 表面年龄为 1009 ± 10Ma,该锆石具有浑圆状的核部,外缘发育有岩浆环带(图 3),其可能是岩浆上升过程中捕获的基底岩浆锆石。

表 1 东塔尔别克和阿希金矿安山岩主量(wt%)和微量元素($\times10^{-6}$)组成

Table 1 Major element (wt%) and trace element ($\times10^{-6}$) compositions of the andesites in east Taerbieke and Axi gold deposit

| 样品号 | 06XJ-30 | 06XJ-31 | 06XJ-32 | 06XJ-33 | wxt818 | wxt819 | wxt821 | AX03 | AX04 | AX14 |
|---|---|---|---|---|---|---|---|---|---|---|
| 岩石类型 | 蚀变安山岩 | 蚀变安山岩 | 安山岩 | 安山岩 | 安山岩 | 安山岩 | 安山岩 | 安山岩 | 安山岩 | 玄武安山岩 |
| 地点 | 东塔尔别克金矿 | | | | 阿希金矿* | | | | | |
| $SiO_2$ | 63.85 | 62.02 | 58.94 | 61.32 | 57.93 | 56.23 | 60.10 | 56.59 | 56.01 | 53.30 |
| $TiO_2$ | 0.48 | 0.67 | 0.81 | 0.77 | 0.72 | 0.74 | 0.68 | 0.87 | 0.88 | 0.95 |
| $Al_2O_3$ | 15.90 | 16.01 | 15.39 | 16.65 | 15.19 | 15.26 | 14.28 | 17.08 | 17.21 | 18.22 |
| $Fe_2O_3$ | 3.77 | 5.03 | 5.91 | 5.28 | 5.36 | 7.26 | 5.38 | 7.10 | 7.15 | 8.06 |
| MnO | 0.05 | 0.07 | 0.10 | 0.11 | 0.06 | 0.07 | 0.07 | 0.09 | 0.08 | 0.08 |
| MgO | 2.51 | 3.79 | 6.59 | 3.75 | 7.65 | 8.47 | 6.78 | 4.56 | 4.04 | 3.36 |
| CaO | 0.70 | 0.98 | 2.51 | 2.18 | 4.90 | 4.38 | 5.88 | 6.98 | 7.21 | 7.21 |
| $Na_2O$ | 2.04 | 4.87 | 4.63 | 6.23 | 2.54 | 2.65 | 2.26 | 2.64 | 2.76 | 3.09 |
| $K_2O$ | 5.92 | 2.17 | 1.64 | 1.04 | 1.76 | 1.45 | 0.66 | 0.85 | 0.64 | 1.08 |
| $P_2O_5$ | 0.08 | 0.08 | 0.11 | 0.10 | 0.08 | 0.06 | 0.07 | 0.18 | 0.18 | 0.23 |
| LOI | 3.99 | 3.75 | 3.72 | 3.03 | 3.36 | 3.92 | 3.20 | 3.08 | 3.95 | 4.11 |
| Total | 99.30 | 99.43 | 100.35 | 100.45 | 99.55 | 100.49 | 99.36 | 103.41 | 103.32 | 103.85 |
| $Mg^{\#}$ | 57.00 | 60.00 | 69.00 | 58.00 | 73.87 | 69.80 | 71.40 | 55.99 | 52.81 | 45.23 |
| Sc | 8.23 | 10.9 | 17.0 | 10.8 | 17.0 | 15.3 | 17.4 | 25.2 | 25.1 | 20.4 |
| V | 75.9 | 72.4 | 94.7 | 76.4 | 117 | 118 | 114 | 177 | 253 | 158 |
| Cr | 60.1 | 70.1 | 241 | 94.2 | 790 | 768 | 789 | 57.4 | 56.4 | 10.3 |
| Co | 11.4 | 16.2 | 22.9 | 18.6 | 26.6 | 27.2 | 26.4 | 19.4 | 20.3 | 21.4 |
| Ni | 35.9 | 37.1 | 126 | 54.5 | 182 | 183 | 186 | 21.2 | 21.0 | 9.20 |
| Ga | 17.6 | 18.7 | 16.8 | 17.5 | 16.1 | 16.1 | 15.1 | 18.5 | 19.0 | 20.2 |
| Cs | 8.18 | 5.72 | 8.11 | 9.06 | | | | 2.12 | 4.12 | 2.76 |
| Rb | 231 | 86.1 | 53.6 | 27.7 | 59.4 | 29.5 | 14.2 | 24.2 | 18.5 | 27.0 |
| Ba | 368 | 345 | 299 | 371 | 295 | 287 | 198 | 214 | 198 | 289 |
| Th | 4.96 | 4.76 | 4.75 | 5.36 | 5.50 | 5.11 | 4.94 | 3.75 | 3.72 | 4.04 |
| U | 1.50 | 1.36 | 1.13 | 1.57 | 1.58 | 1.37 | 1.23 | 1.06 | 1.09 | 1.07 |
| Pb | 6.36 | 7.45 | 8.20 | 6.08 | 12.2 | 11.4 | 8.47 | 8.94 | 8.83 | 7.97 |
| Nb | 5.83 | 6.92 | 9.07 | 9.53 | 6.02 | 5.74 | 5.35 | 6.84 | 6.96 | 13.3 |
| Ta | 0.471 | 0.559 | 0.705 | 0.746 | 0.536 | 0.473 | 0.444 | 0.510 | 0.510 | 0.620 |
| Sr | 235 | 354 | 686 | 697 | 297 | 294 | 317 | 353 | 387 | 365 |
| Y | 9.86 | 12.2 | 14.3 | 14.8 | 17.4 | 17.2 | 16.6 | 20.5 | 21.7 | 21.3 |
| Zr | 149 | 176 | 159 | 168 | 128 | 114 | 109 | 122 | 125 | 171 |
| Hf | 3.66 | 4.19 | 3.61 | 3.87 | 3.58 | 3.08 | 2.91 | 3.64 | 3.65 | 3.94 |
| La | 13.6 | 12.7 | 13.4 | 14.1 | 11.3 | 11.5 | 11.1 | 15.8 | 15.6 | 19.6 |
| Ce | 27.4 | 28.1 | 27.6 | 29.0 | 24.8 | 23.4 | 24.6 | 33.1 | 33.1 | 40.4 |
| Pr | 3.19 | 3.42 | 3.33 | 3.48 | 3.07 | 2.86 | 2.95 | 4.21 | 4.23 | 5.06 |
| Nd | 11.5 | 12.8 | 12.6 | 13.2 | 12.2 | 11.1 | 11.6 | 17.1 | 17.5 | 19.8 |
| Sm | 2.18 | 2.71 | 2.74 | 2.76 | 2.77 | 2.52 | 2.54 | 3.83 | 3.98 | 4.17 |
| Eu | 0.601 | 0.736 | 0.884 | 0.878 | 0.930 | 0.932 | 0.869 | 1.07 | 1.08 | 1.23 |
| Gd | 1.86 | 2.34 | 2.56 | 2.66 | 2.85 | 2.67 | 2.64 | 3.84 | 3.95 | 4.23 |
| Tb | 0.300 | 0.368 | 0.428 | 0.425 | 0.470 | 0.456 | 0.434 | 0.600 | 0.610 | 0.610 |
| Dy | 1.70 | 2.06 | 2.54 | 2.59 | 3.02 | 2.84 | 2.75 | 3.61 | 3.78 | 3.74 |
| Ho | 0.366 | 0.445 | 0.513 | 0.537 | 0.602 | 0.585 | 0.566 | 0.770 | 0.810 | 0.780 |
| Er | 1.07 | 1.25 | 1.49 | 1.55 | 1.62 | 1.64 | 1.55 | 2.14 | 2.23 | 2.15 |
| Tm | 0.167 | 0.183 | 0.207 | 0.228 | 0.268 | 0.262 | 0.248 | 0.330 | 0.340 | 0.330 |
| Yb | 1.12 | 1.24 | 1.53 | 1.59 | 1.66 | 1.69 | 1.64 | 2.08 | 2.12 | 2.02 |
| Lu | 0.175 | 0.199 | 0.222 | 0.232 | 0.283 | 0.264 | 0.265 | 0.300 | 0.320 | 0.310 |

* 阿希金矿火山岩数据来自王强等(2006)和龙灵利等(2008)

**表 2　东塔尔别克安山岩锆石 LA-ICP-MS 分析结果**

Table 2　Zircon LA-ICP-MS analyzing results for the east Taerbieke andesite

| 分析点号 | 元素含量($\times10^{-6}$) | | 元素比值 | 同位素比值 | | | | | | 表观年龄(Ma) | | | | | |
|---|---|---|---|---|---|---|---|---|---|---|---|---|---|---|---|
| | Th | U | U/Th | $^{207}Pb/^{206}Pb$ | $1\sigma$ | $^{207}Pb/^{235}U$ | $1\sigma$ | $^{206}Pb/^{238}U$ | $1\sigma$ | $^{207}Pb/^{206}Pb$ | $1\sigma$ | $^{207}Pb/^{235}U$ | $1\sigma$ | $^{206}Pb/^{238}U$ | $1\sigma$ |
| 06XJ31-1 | 139 | 242 | 1.74 | 0.05366 | 0.00089 | 0.4138 | 0.00691 | 0.05593 | 0.00063 | 357 | 37 | 352 | 5 | 351 | 4 |
| 06XJ31-2 | 83 | 136 | 1.64 | 0.05639 | 0.00124 | 0.43478 | 0.00949 | 0.05592 | 0.00066 | 467 | 48 | 367 | 7 | 351 | 4 |
| 06XJ31-3 | 84 | 130 | 1.55 | 0.0545 | 0.00108 | 0.41928 | 0.00832 | 0.0558 | 0.00064 | 392 | 44 | 356 | 6 | 350 | 4 |
| 06XJ31-4 | 87 | 128 | 1.47 | 0.05466 | 0.0012 | 0.42163 | 0.00922 | 0.05595 | 0.00066 | 398 | 48 | 357 | 7 | 351 | 4 |
| 06XJ31-5 | 139 | 255 | 1.83 | 0.05299 | 0.0009 | 0.40842 | 0.007 | 0.05591 | 0.00063 | 328 | 38 | 348 | 5 | 351 | 4 |
| 06XJ31-6 | 53 | 175 | 3.30 | 0.07392 | 0.00104 | 1.72725 | 0.02481 | 0.16948 | 0.00188 | 1039 | 28 | 1019 | 9 | 1009 | 10 |
| 06XJ31-7 | 147 | 201 | 1.37 | 0.05493 | 0.00095 | 0.41996 | 0.00731 | 0.05545 | 0.00062 | 409 | 38 | 356 | 5 | 348 | 4 |
| 06XJ31-8 | 111 | 169 | 1.52 | 0.05478 | 0.00098 | 0.42285 | 0.00764 | 0.05599 | 0.00063 | 403 | 39 | 358 | 5 | 351 | 4 |
| 06XJ31-9 | 26 | 41 | 1.55 | 0.05581 | 0.00252 | 0.55185 | 0.02446 | 0.07172 | 0.00108 | 445 | 97 | 446 | 16 | 447 | 6 |
| 06XJ31-10 | 107 | 156 | 1.46 | 0.05135 | 0.00095 | 0.39074 | 0.00727 | 0.05519 | 0.00063 | 256 | 42 | 335 | 5 | 346 | 4 |
| 06XJ31-11 | 145 | 218 | 1.51 | 0.05343 | 0.00092 | 0.40663 | 0.00707 | 0.0552 | 0.00062 | 347 | 39 | 346 | 5 | 346 | 4 |
| 06XJ31-12 | 74 | 147 | 2.00 | 0.05303 | 0.00112 | 0.40504 | 0.00851 | 0.05539 | 0.00064 | 330 | 47 | 345 | 6 | 348 | 4 |
| 06XJ31-13 | 116 | 201 | 1.73 | 0.05358 | 0.00107 | 0.40066 | 0.00799 | 0.05424 | 0.00062 | 353 | 45 | 342 | 6 | 341 | 4 |
| 06XJ31-14 | 56 | 90 | 1.61 | 0.05303 | 0.00137 | 0.40129 | 0.01027 | 0.05488 | 0.00066 | 330 | 58 | 343 | 7 | 344 | 4 |
| 06XJ31-15 | 66 | 117 | 1.77 | 0.05164 | 0.00129 | 0.38856 | 0.00961 | 0.05457 | 0.00065 | 270 | 56 | 333 | 7 | 343 | 4 |
| 06XJ31-16 | 115 | 179 | 1.55 | 0.05407 | 0.00122 | 0.40569 | 0.00913 | 0.05442 | 0.00064 | 374 | 50 | 346 | 7 | 342 | 4 |
| 06XJ31-17 | 68 | 116 | 1.71 | 0.05398 | 0.00145 | 0.41253 | 0.01098 | 0.05543 | 0.00068 | 370 | 59 | 351 | 8 | 348 | 4 |
| 06XJ31-18 | 59 | 126 | 2.15 | 0.05274 | 0.00131 | 0.39694 | 0.00974 | 0.05459 | 0.00065 | 318 | 55 | 339 | 7 | 343 | 4 |
| 06XJ31-19 | 84 | 153 | 1.81 | 0.0566 | 0.00123 | 0.43331 | 0.00939 | 0.05552 | 0.00065 | 475 | 48 | 366 | 7 | 348 | 4 |
| 06XJ31-20 | 31 | 82 | 2.61 | 0.05839 | 0.00245 | 0.43571 | 0.0179 | 0.05412 | 0.00079 | 545 | 89 | 367 | 13 | 340 | 5 |
| 06XJ31-21 | 162 | 304 | 1.87 | 0.05374 | 0.00098 | 0.41202 | 0.00756 | 0.05561 | 0.00063 | 360 | 40 | 350 | 5 | 349 | 4 |
| 06XJ31-22 | 144 | 286 | 1.98 | 0.05411 | 0.00098 | 0.41449 | 0.0075 | 0.05556 | 0.00063 | 375 | 40 | 352 | 5 | 349 | 4 |
| 06XJ31-23 | 52 | 105 | 2.03 | 0.05161 | 0.0012 | 0.39316 | 0.00908 | 0.05525 | 0.00065 | 268 | 52 | 337 | 7 | 347 | 4 |
| 06XJ31-24 | 71 | 150 | 2.11 | 0.05277 | 0.00108 | 0.40516 | 0.00825 | 0.05568 | 0.00064 | 319 | 46 | 345 | 6 | 349 | 4 |
| 06XJ31-25 | 204 | 320 | 1.57 | 0.05363 | 0.00097 | 0.40969 | 0.00744 | 0.05541 | 0.00063 | 355 | 41 | 349 | 5 | 348 | 4 |

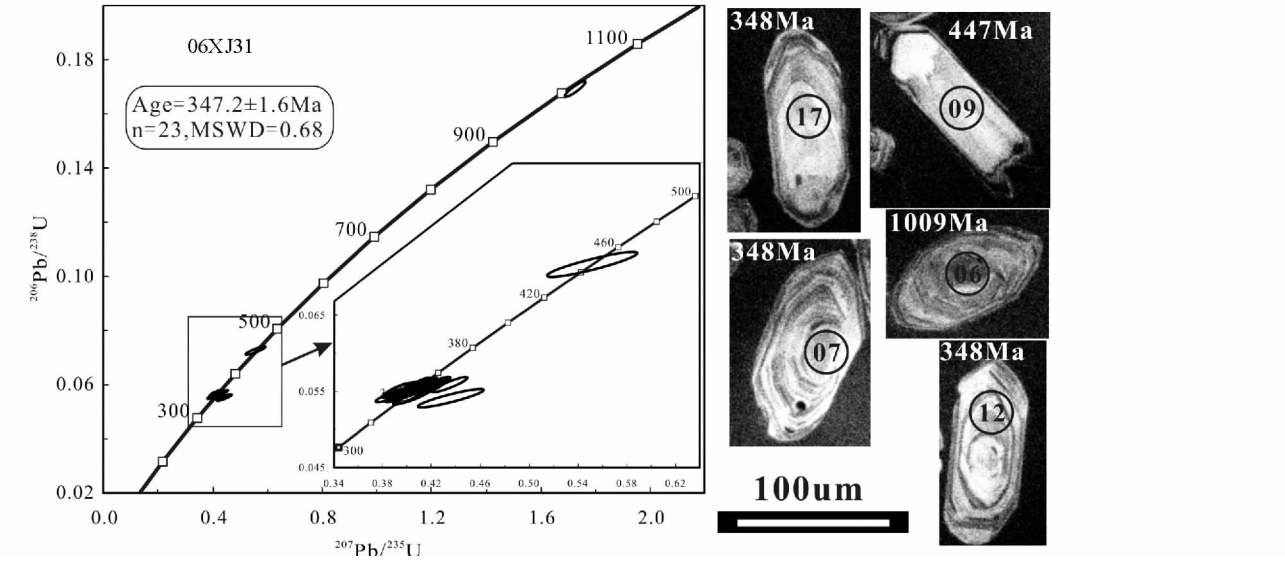


图 3 06XJ31 LA-ICP-MS 锆石 U-Pb 谐和图和锆石 CL 图像

Fig. 3 LA-ICP-MS zircon U-Pb concordia diagrams and zircon cathodoluminescence (CL) images

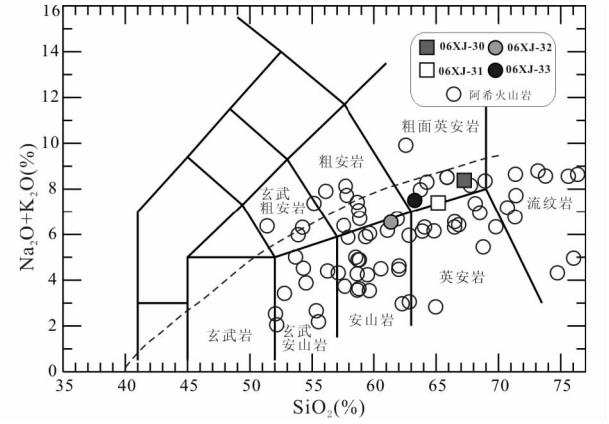


图 4 TAS 图解(据 Le Maitre, 2002)

阿希火山岩数据来自左学义等,2005; 沙德铭等, 2005; 王强等, 2006; 龙灵利等, 2008

Fig. 4 TAS digram (after Le Maitre, 2002)

### 4.2 元素地球化学特征

我们对东塔尔别克四件安山岩进行了全岩地球化学分析。其中样品 06XJ-30 和 06XJ-31 两样品取自靠近矿化带处,岩石有蚀变,而 06XJ-32 和 06XJ-33 两样品取自远离矿化带的地方,较新鲜。安山岩的 $SiO_2$ 含量在 58.94% ~ 63.85%,变化范围较小;具有较高的 MgO 含量(2.51% ~ 6.59%)和高的 $Mg^{\#}$(57 ~ 69);全碱的含量为 6.27% ~ 7.96%;$Al_2O_3$ 含量较高(15.39% ~ 16.65%)。安山岩在 TAS 图解(图 4)中落入亚碱性范围内,在 $SiO_2$-$FeO^T$/MgO 图中(图 5a)均落入钙碱性区域。

安山岩稀土元素分布模式为轻稀土富集型,轻重稀土分馏明显(图 6a);无明显 Eu 异常($\delta$Eu 为 0.89 ~ 1.02),但重稀土元素分异不明显,$(Gd/Yb)_N$ = 1.37 ~ 1.56;富集大离子亲石元素(LILE),如 Sr 具有明显的正异常,亏损高场强元素(HFSE)和重稀土元素,Nb、Ti 有明显的负异常(图 6b)。以上这些特点显示它们与俯冲带岩浆地球化学特征类似(Wilson, 1989)。

## 5 讨论

### 5.1 形成时代

前人曾对西天山与铜金相关的岩浆岩的年代学进行了深入研究。但目前对该区出露的岩浆岩的形成时代仍有争议:李华芹(1998)用 Rb-Sr 等时线法测得阿希金矿赋矿围岩大哈拉军山组火山岩的年龄为 346 ~ 321Ma,为早石炭世;Zhu *et al.* (2005))给出分布于西南天山大哈拉军山组火山岩的 SHRIMP 锆石年龄分别为 353.7 ± 4.5Ma 和 312.8 ± 4.2Ma 的资料,分别属于早石炭世和晚石炭世;翟伟等(2006)报道了阿希金矿床赋矿围岩大哈拉军山组火山岩 SHRIMP 锆石年龄为 363.2 ± 5.7Ma,但没有对岩石中出现的年轻锆石(342 ~ 327Ma)给予解释。本次对东塔尔别克矿区的花岗闪长斑岩的定年结果显示其结晶年龄为 347.2 ± 1.6Ma,这与阿希金矿赋矿安山岩的 SHRIMP 锆石 U-Pb 年龄(356 ~ 342Ma,王强未发表数据)相一致,也与该区地层古生物的证据(王福同, 2006)一致。因此,我们认为东塔尔别克岩浆岩形成于早石炭世。

### 5.2 岩石类型与成因

东塔尔别克的安山岩与阿希金矿区的火山岩相似(图 4 ~ 8),其具有高的 MgO 含量和 $Mg^{\#}$、高的 Cr($60.1 \times 10^{-6}$ ~

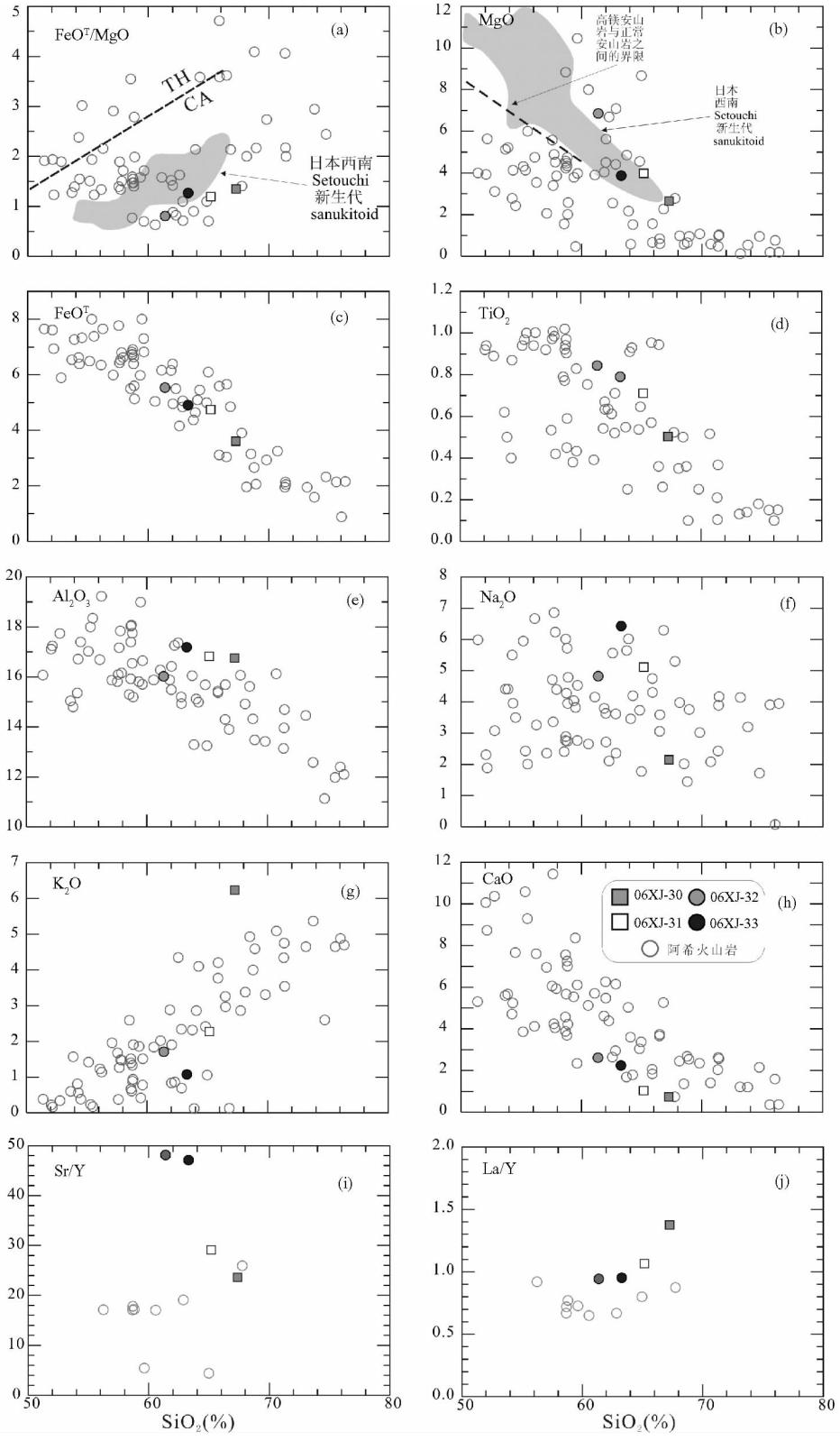


图 5　$SiO_2$ 对 $FeO^T/MgO$（a）、MgO（b）、FeO（c）、$TiO_2$（d）、$Al_2O_3$（e）、$Na_2O$（f）、$K_2O$（g）、CaO（h）、Sr/Y（i）和 La/Y（j）图

（a）中 TH-拉斑系列；CA-钙碱系列；（b）高镁安山岩与正常安山岩分界线来源于 McCarron and Smellie（1998）；日本西南 Setouchi 新生代 Sanukitoid 来源于 Tatsumi（2006）；阿希火山岩数据来自左学义等（2005）、沙德铭等（2005）、王强等（2006）和龙灵利等（2008）

Fig. 5　$SiO_2$ versus $FeO^T/MgO$（a）, MgO（b）, FeO（c）, $TiO_2$（d）, $Al_2O_3$（e）, $Na_2O$（f）, $K_2O$（g）, CaO（h）, Sr/Y（i）and La/Y（j）diagrams

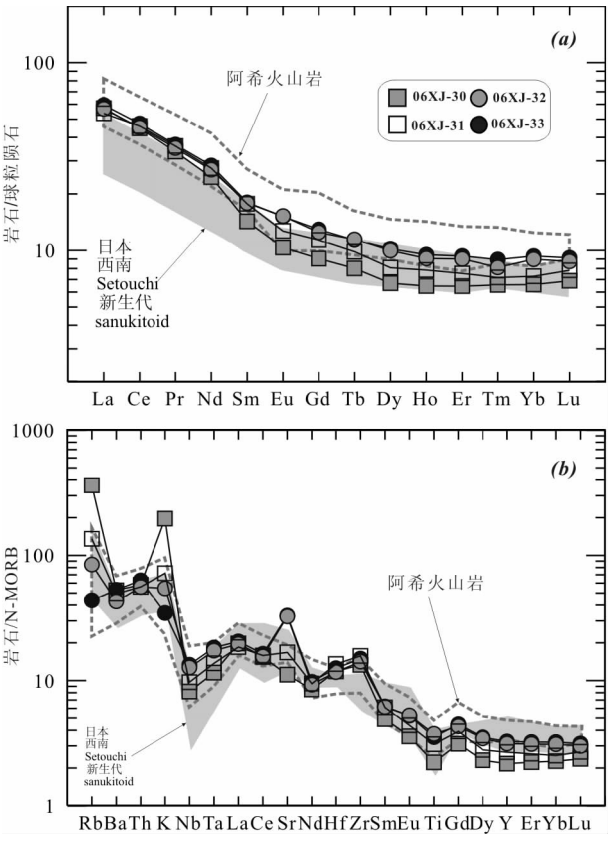


图 6 稀土元素球粒陨石标准化配图(a)和微量元素 NMORB 标准化蛛网图(b)(标准值据 Sun and McDonough, 1989)

阿希火山岩数据来自王强等(2006)和龙灵利等(2008)

Fig. 6 The chondrite-normalized rare earth element (REE) patterns (a) and primitive mantle-normalized multi-element plots (b) (normalized values from, Sun and McDonough, 1989)

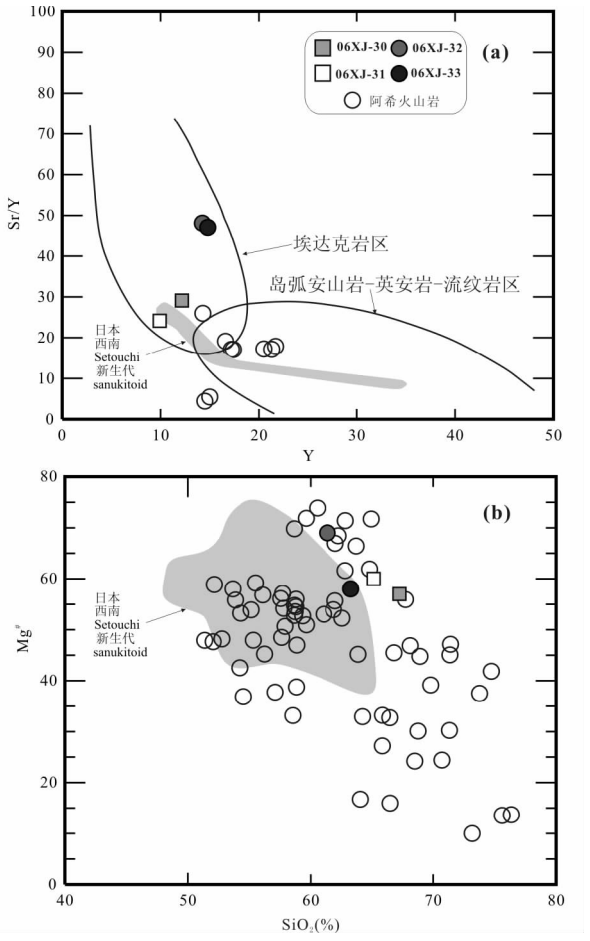


图 7 Sr/Y-Y (a, Defant and Drummond, 1993)和 $SiO_2$-$Mg^{\#}$(b)

图解数据来源同图 4

Fig. 7 Sr/Y-Y (a, after Defant and Drummond, 1993) and $SiO_2$-$Mg^{\#}$(b) diagrams

$241\times10^{-6}$)和 Ni($35.9\times10^{-6}\sim126\times10^{-6}$)含量,以及低的 $FeO^T/MgO$,类似于高镁安山岩(Polat and Kerrich, 2001; Tatsumi, 2001)。但同时与阿希金矿的火山岩相比,东塔尔别克安山岩具有埃达克岩的特征(Defant and Drummond, 1990):无明显 Eu 异常,其中两新鲜样品具有高的 Sr 含量($685\times10^{-6}\sim696\times10^{-6}$)和低 Y 含量($14.3\times10^{-6}\sim14.9\times10^{-6}$),以及高的 Sr/Y 比值(47.1~48.1),在 Sr-Y 判别图(图 7a)(Defant and Drummond, 1993)中均落入埃达克区。而两蚀变的样品具有相对低的 Sr 含量($235\times10^{-6}\sim354\times10^{-6}$)和高的 $K_2O$(2.17%~5.92%)含量(表 1),很可能与蚀变有关。所以东塔尔别克的安山岩为高镁安山岩-埃达克岩组合。

目前,对埃达克质岩浆的形成提出了不同的机制,主要包括:(1)俯冲洋壳熔融(Defant and Drummond, 1990; Zhang *et al.*, 2004, 2006b; Han *et al.*, 2006);(2)增厚下地壳熔融(Atherton and Petford, 1993; Wang *et al.*, 2005; Zhang *et al.*, 2006a; Lai *et al.*, 2007; Xiao and Clemens, 2007; Zhao *et al.*, 2008; 张旗等, 2001);(3)拆沉下地壳熔融(Kay and Kay, 1993; Xu *et al.*, 2002; Gao *et al.*, 2004; Wang *et al.*, 2006a, 2007a; Hou *et al.*, 2007; Huang *et al.*, 2008; Liu S *et al.*, 2008);(4)玄武质岩浆的结晶分异(Castillo *et al.*, 1999; Macpherson *et al.*, 2006)。在玄武质岩浆的结晶分异过程中,石榴石±辉石的高压分离结晶作用导致岩浆中的 $Al_2O_3$ 随着 $SiO_2$ 的增加而降低,而 Sr/Y, La/Y 比值则随 $SiO_2$ 的增加而升高,但东塔尔别克岩浆岩没有这样的规律性变化(图 5i, j),所以其不可能由玄武质岩浆的结晶分异所形成。同时东塔尔别克岩浆岩的具有高的 MgO 和 $Mg^{\#}$(57~69),所以排除(2)的可能性。由于拆沉下地壳熔融往往发生在板内伸展环境(Xu *et al.*, 2002; Gao *et al.*, 2004; Wang *et al.*, 2006a),这与西天山北部早石炭世的构造背景不符。最近的研究表明,在天山北部地区存在石炭纪洋壳的俯冲和熔融作用,并且形成了典型的岛弧岩浆岩组合:埃达克岩-高镁安山

岩-富 Nb 玄武岩组合(Wang *et al.*, 2007b; 王强等, 2006)。因此,我们认为东塔尔别克高镁埃达克岩岩浆的形成更可能与洋壳的俯冲有关,可能是由俯冲洋壳熔融所形成,同时其高的 MgO 含量和 $Mg^{\#}$暗示可能受到地幔橄榄岩的混染。

早期含水地幔橄榄岩熔融实验表明,在大多数情况下地幔橄榄岩的熔融一般都是形成玄武质岩石,尤其在高温和高压的情况下更是如此。但含水地幔橄榄岩在低温低压情况下的熔融(约 1000℃,1GPa)是产生高镁安山质岩浆的一种可能机制(如 Kushiro, 1969; Tatsumi and Ishizaka, 1981, 1982)。这些实验结果使 Crawford *et al.* (1989)和 Tatsumi and Maruyama (1989)认为:高镁安山岩可能是由俯冲的洋壳释放的含水流体加入到地幔楔中而引发地幔橄榄岩熔融形成的。Hirose(1997)通过直接熔融含水地幔橄榄岩实验进一步表明,高镁安山岩只能在低于 1300℃、压力为 1GPa 且含水条件下形成。但最近的一系列的研究表明有些高镁安山岩更有可能是由俯冲洋壳(+沉积物)熔融的硅质熔体和上覆的地幔橄榄岩相互反应所形成,尤其是日本西南 Setouchi 火山岩带中的 Sanukitoid(赞岐岩类)(Shimoda *et al.*, 1998; Tatsumi, 2001; Hanyu *et al.*, 2002, 2006; Tatsumi and Hanyu, 2003)。

赞岐岩最早是指在日本四国东北 Sanuki 地区的灰-黑色、有光泽、隐晶质致密的含有针状古铜辉石斑晶的火山岩(Tatsumi, 2006)。Koto (1916)进一步将日本西南新生代 Setouchi 火山岩带中与赞岐岩相似且为黑色、斑晶 < 10% 的致密火山岩称为赞岐岩类(Sanukitoid)。Tatsumi and Ishizaka (1981,1982)则将"赞岐岩类"的概念用于 Setouchi 火山岩带中那些斑晶少于 10%(没有或很少有斜长石斑晶)和无斑隐晶的高镁玄武岩-安山岩,岩石类型包括普通辉石橄榄玄武岩、普通辉石橄榄安山岩、古铜辉石橄榄安山岩和古铜辉石安山岩。后来,Shirey and Hanson(1984)、Stern and Hanson (1991)、Smithies and Champion(2000)和 Martin *et al.* (2005)将太古宙具上述赞岐岩特征(Si 过饱和、$Mg^{\#}$和 Ni、Cr、LILE 含量高)的深成岩和火山岩(高镁二长闪长岩、花岗闪长岩和粗安岩)称为"赞岐岩类"。东塔尔别克的含普通辉石安山岩的地球化学特征有些类似于赞岐岩,在 Th/La-Th 图解中(图 8)东塔尔别克安山岩落入 Setouchi 的赞岐岩区域,由于其高的 Th/La 比和 Th 含量,其源区可能包含了更多俯冲洋壳上覆沉积物熔体成分,即由洋壳和沉积物的熔体与地幔橄榄岩相互作用的结果。

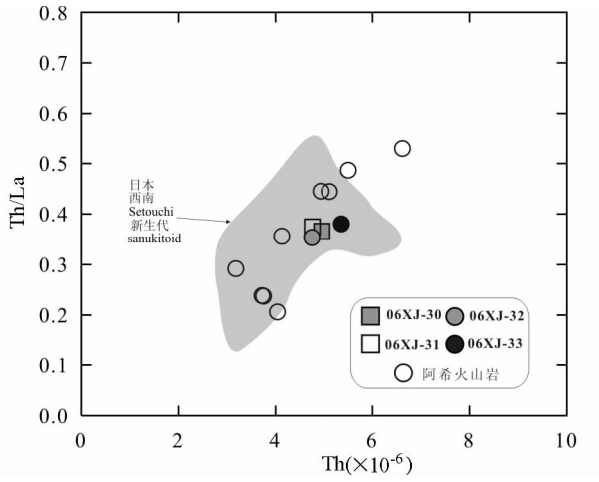


图 8　Th/La-Th 图解

阿希火山岩数据来自王强等(2006)和龙灵利等(2008)

Fig. 8　Th/La-Th diagram

## 5.3　动力学与成矿意义

### 5.3.1　动力学背景

目前,西天山北缘石炭纪火山岩的形成模式主要包括有以下三种:(1)裂谷(Xia *et al.*, 2004b;车自成和刘良, 1996);(2)地幔柱(夏林圻等,2004);(3)俯冲岛弧环境(Gao *et al.*, 1998; Zhang *et al.*, 2003; Liu and Fei, 2006; Wang *et al.*, 2007b; Xiao *et al.*, 2008; Qian *et al.*, 2009; 王强等, 2006; 李锦轶等, 2006; 龙灵利等, 2008)。最近,王强等(2006)在天山北部地区厘定出典型的岛弧岩浆岩组合:埃达克岩-高镁安山岩-富 Nb 玄武岩组合,并认为可能是与石炭纪洋壳的俯冲和熔融有关。龙灵利等(2008)等认为伊犁板块南北缘石炭纪火山岩类似于俯冲带之上大陆边缘火山岛弧岩特征,可能是大陆边缘环境下的产物。随着详细的岩石学和地球化学研究的深入,越来越多的数据显示该区的火山岩以钙碱性为主,碱性岩很少。另外,西天山的中基性熔岩的时代为 354 ~ 313Ma,时限大于 40Ma,该区火山岩并具有典型大陆弧岩浆的地球化学特征(Zhu *et al.*, 2005)。本文资料表明,东塔尔别克的安山岩也类似于俯冲带岩浆地球化学特征(Wilson, 1989)。所以,我们趋向认为西天山北缘在早石炭世为岛弧环境。

### 5.3.2　成矿意义

高镁安山岩-埃达克岩型岩浆岩对于该区的 Au 的成矿作用具有重要意义:(1)Au 是亲硫元素,主要赋存于地幔和铁镁质岩石,所以玄武质洋壳熔融形成的埃达克岩具有良好的成矿物质来源;(2)板片熔体具有高的氧逸度(Mungall, 2002),Mungall (2002)认为板片熔体可以携带大量的 $Fe_2O_3$,当携带大量 $Fe_2O_3$的板片熔体进入到富金属硫化物的地幔楔时,将会导致地幔楔橄榄岩氧逸度($f_{O2}$)的增高,地幔中的金属硫化物将被氧化,Au 等将顺利进入到板片熔体或岛弧岩浆中;安山岩高的 MgO 含量和 $Mg^{\#}$就是板片熔体与地幔橄榄岩相互作用的证据;(3)俯冲板片富含挥发份 $H_2O$ 和 Cl,挥发份 Cl 在高温高压下是 Au 等金属元素的强烈配合剂,它们将与 Au 形成稳定的配合物随岩浆一起迁移,有利于成矿(熊小林等, 2005)。东塔尔别克金矿北据阿希金矿仅 2km,与其共生的岩浆岩与阿希金矿火山岩相似,同时其形成时代也一致。二者的成矿机制可能相同,甚至东塔尔别克金矿很可能是阿希金矿向南延伸的部分。

## 6 结论

(1)东塔尔别克安山岩的形成时代为 347.2 ± 1.6Ma,形成于早石炭世岛弧环境。

(2)东塔尔别克岩浆岩为高镁安山岩-埃达克岩组合,其形成可能是与洋壳的俯冲熔融作用所形成,同时可能包含了更多俯冲洋壳上覆沉积物熔体成分,即由洋壳和沉积物的熔体与地幔橄榄岩相互作用的结果。

(3)俯冲带熔体与地幔的作用对于区内金矿的形成可能具有重要的意义。

**致谢** 感谢朱永峰教授和匿名审稿人对本文的初稿提出了宝贵意见。室内主量、微量元素分析得到了刘颖、胡光黔老师的帮助,锆石年代学分析得到了刘勇胜教授和宗克清的帮助,在此一并表示感谢!

## References

Allen MB, Windley BF and Zhang C. 1993. Palaeozoic collisional tectonics and magmatism of the Chinese Tien Shan, central Asia. Tectonophysics, 220(1-4): 89-115

Atherton MP and Petford N. 1993. Generation of sodium-rich magmas from newly underplated basaltic crust. Nature, 362(6416): 144-146

Castillo PR, Janney PE and Solidum RU. 1999. Petrology and geochemistry of Camiguin Island, southern Philippines: Insights to the source of adakites and other lavas in a complex arc setting. Contributions to Mineralogy and Petrology, 134(1): 33-51

Che ZL and Liu L. 1996. Review on the Ancient Yili Rift, Xinjiang, China. Acta Petrologica Sinica, 12(3): 478-490(in Chinese with English abstract)

Coleman RG. 1989. Continental growth of Northwest China. Tectonics, 8(3): 621-635

Crawford AJ, Falloon TJ and Green DH. 1989. Classification, petrogenesis and tectonic setting of boninites. In: Crawford AJ (ed.). Boninites and Related Rocks. Unwin Hyman, Unwin Hyman, 1-49

Defant MJ and Drummond MS. 1990. Derivation of some modern arc magmas by melting of young subducted lithosphere. Nature, 347(6294): 662-665

Defant MJ and Drummond MS. 1993. Mount St. Helens: Potential example of the partial melting of the subducted lithosphere in a volcanic arc. Geology, 21(6): 547-550

Gao J, Li MS, Xiao XC, Tang YQ and He GQ. 1998. Paleozoic tectonic evolution of the Tianshan Orogen, northwestern China. Tectonophysics, 287(1-4): 213-231

Gao S, Rudnick RL, Yuan HL, Liu XM, Liu YS, Xu WL, Ling WL, Ayers J, Wang XC and Wang QH. 2004. Recycling lower continental crust in the North China craton. Nature, 432(7019): 892-897

Han CM, Xiao WJ, Zhao GC, Mao JW, Yang JM, Wang ZL, Yan Z and Mao QG. 2006. Geological characteristics and genesis of the Tuwu porphyry copper deposit, Hami, Xinjiang, Central Asia. Ore Geology Reviews, 29(1): 77-94

Hanyu T, Tatsumi Y and Nakai S. 2002. A contribution of slab-melts to the formation of high-Mg andesite magmas: Hf isotopic evidence from SW Japan. Geophysical Research Letters, 29(22) doi:10.1029/2001GL015856

Hanyu T, Tatsumi Y, Nakai S, Chang Q, Miyazaki T, Sato K, Tani K, Shibata T and Yoshida T. 2006. Contribution of slab melting and slab dehydration to magmatism in the NE Japan arc for the last 25 Myr: Constraints from geochemistry. Geochemistry Geophysics Geosystems, 7(8) doi:10.1029/2005GC001220

Hirose K. 1997. Melting experiments on lherzolite KLB-1 under hydrous conditions and generation of high-magnesian andesitic melts. Geology, 25(1): 42-44

Hou ML, Jiang YH, Jiang SY, Ling HF and Zhao K. 2007. Contrasting origins of Late Mesozoic adakitic granitoids from the northwestern Jiaodong Peninsula, east China: Implications for crustal thickening to delamination. Geological Magazine, 144(4): 619-631

Huang F, Li SG, Dong F, He YS and Chen FK. 2008. High-Mg adakitic rocks in the Dabie orogen, central China: Implications for foundering mechanism of lower continental crust. Chemical Geology, 255(1-2): 1-13

Jia B, Wu RS, Tian CL, Sha, DM, Yang S. 2001. The characteristics of tawuerbieke - abiyindi porphyry type of gold deposit. Geology and Resources, 10(3): 139-145(in Chinese with English abstract)

Kay RW and Kay SM. 1993. Delamination and delamination magmatism. Tectonophysics, 219(1-3): 177-189

Koto B. 1916. On the volcanoes of Japan (V). J. Geol. Soc. Tokyo, 23: 95-127

Kushiro I. 1969. The system forsterite-diopside-silica with and without water at high pressures. American Journal of Science, 269-294

Lai SC, Qin JF and Li YF. 2007. Partial melting of thickened Tibetan crust: Geochemical evidence from Cenozoic adakitic volcanic rocks. International Geology Review, 49(4): 357-373

Le Maitre RW. 2002. Igneous Rocks: A Classification and Glossary of Terms. Cambridge: Cambridge University Press, 236

Li HQ. 1998. Study on Metallogenetic Chronology of Nonferrous and Precious Metallic Ore Deposits in Northern Xinjiang, China. Beijing: Geological Publishing House (in Chinese with English abstract)

Li HQ, Wang DH, Wan Y, Qu WJ, Zhang B, Lu YF, Mei YP and Zou SL. 2006a. Isotopic geochronology study and its significance of the Lailisigao'er Mo deposit, Xinjiang. Acta Petrologica Sinica, 22(10): 2437-2443(in Chinese with English abstract)

Li JY, Wang KZ, Sun GH, Mo SG, Li WQ, Yang TN and Gao LM. 2006b. Paleozoic active margin slices in the southern Turfan-Hami basin: Geological records of subduction of the Paleo-Asian Ocean plate in central Asian regions. Acta Petrologica Sinica, 22(5): 1087-1102(in Chinese with English abstract)

Li XH. 1997. Geochemistry of the Longsheng ophiolite from the southern margin of Yangtze Craton, SE China. Geochemical Journal, 31: 323-327

Li XH, Qi CS, Liu Y, Liang XR, Tu XL, Xie LW and Yang YH. 2005. Petrogenesis of the Neoproterozoic bimodal volcanic rocks along the western margin of the Yangtze Block: New constraints from Hf isotopes and Fe/Mn ratios. Chinese Science Bulletin, 50(21): 2481-2486

Liu S, Hu RZ, Feng CX, Zou HB, Li CAI, Chi XG, Peng JT, Zhong H, Qi L, Qi YQ and Wang T. 2008. Cenozoic high Sr/Y volcanic rocks in the Qiangtang terrane, northern Tibet: Geochemical and isotopic evidence for the origin of delaminated lower continental melts. Geological Magazine, 145(4): 463-474

Liu W and Fei PX. 2006. Methane-rich fluid inclusions from ophiolitic dunite and post-collisional mafic-ultramafic intrusion: The mantle dynamics underneath the Palaeo-Asian Ocean through to the post-collisional period. Earth and Planetary Science Letters, 242(3-4): 286-301

Liu YS, Hu ZC, Gao S, G ntherr D, Xu J, Gao CG and Chen HH. 2008. In situ analysis of major and trace elements of anhydrous minerals by LA-ICP-MS without applying an internal standard. Chemical Geology, 257(1-2): 34-43

Long LL, Gao J, Qian Q, Xiong XM, Wang JB, Wang YW and Gao LM. 2008. Geochemical charactersitics and tectonic setting of Carboniferous volcanic rocks form Yili region, western Tianshan.

Acta Petrologica Sinica, 24(4): 699 – 710(in Chinese with English abstract)

Ludwig KR. 2003. User's manual for Isoplot 3.00: A geochronological toolkit for Microsoft Excel. Berkeley Geochronology Center Special Publication, 4: 1 – 70

Martin H, Smithies RH, Rapp R, Moyen JF and Champion D. 2005. An overview of adakite, tonalite trondhjemite granodiorite (TTG), and sanukitoid: Relationships and some implications for crustal evolution. Lithos, 79(1 – 2): 1 – 24

Macpherson CG, Dreher ST and Thirlwall MF. 2006. Adakites without slab melting: High pressure differentiation of island arc magma, Mindanao, the Philippines. Earth and Planetary Science Letters, 243(3 – 4): 581 – 593

McCarron JJ and Smellie JL. 1998. Tectonic implications of fore-arc magmatism and generation of high-magnesian andesites: Alexander Island, Antarctica. Journal of the Geological Society, 155: 269 – 280

Mungall JE, 2002. Roasting the mantle: Slab melting and the genesis of major Au and Au-rich Cu deposits. Geology, 915 – 918

Polat A and Kerrich R. 2001. Magnesian andesites, Nb-enriched basalt-andesites, and adakites from Late-Archean 2.7 Ga Wawa greenstone belts, Superior Province, Canada: Implications for Late Archean subduction zone petrogenetic processes. Contributions to Mineralogy and Petrology, 141(1): 36 – 52

Qian Q, Gao J, Klemd R, He G, Song B, Liu D and Xu R. 2009. Early Paleozoic tectonic evolution of the Chinese South Tianshan Orogen: constraints from SHRIMP zircon U-Pb geochronology and geochemistry of basaltic and dioritic rocks from Xiate, NW China. International Journal of Earth Sciences. DOI 10.1007/s00531 – 007 – 0268 – x (in press)

Qin KZ, Sun S, Li JL, Fang TH, Wang SL and Liu W. 2002. Paleozoic epithermal Au and porphyry Cu deposits in North Xinjiang, China: Epochs, features, tectonic linkage and exploration significance. Resource Geology, 52(4): 291 – 300

Rui ZY, Goldfarb RJ, Qiu YM, Zhou TH, Chen RY, Pirajno F and Yun G. 2002. Paleozoic-Early Mesozoic gold deposits of the Xinjiang Autonomous Region, northwestern China. Mineralium Deposita, 37(3): 393 – 418

Sengör AMC, Natal'in BA and Burtman VS. 1993. Evolution of the Altaid tectonic collage and Palaeozoic crustal growth in Eurasia. Nature, 364(6435): 299 – 307

Sha DM, Jin CZ, Dong LH, Wu RS, Tian CL and Jia B. 2005. Study on the metallogenic geochemistry of Axi gold deposit in western Tianshan mountains. Geology and Resources, 14(2): 118 – 125(in Chinese with English abstract)

Shi YS, Lu HF and Jia D. 1994. Paleozoic plate-tectonic evolution of the Tarim and western Tianshan regions, western China. International Geology Review, 36(11): 1058 – 1066

Shirey SB and Hanson GN. 1984. Mantle-derived Archean monzodiorites and trachyandesites. Nature, 310(10): 222 – 224

Shimoda G, Tatsumi Y, Nohda S, Ishizaka K and Jahn BM. 1998. Setouchi high-Mg andesites revisited: Geochemical evidence for melting of subducting sediments. Earth and Planetary Science Letters, 160(3 – 4): 479 – 492

Smithies RH and Champion DC. 2000. The Archaean high-Mg diorite suite: Links to tonalite trondhjemite - granodiorite magmatism and implications for Early Archaean crustal growth. Journal of Petrology, 41(12): 1653 – 1671

Stern RA and Hanson GN. 1991. Archean high-Mg granodiorite: A derivative of light rare earth element-enriched monzodiorite of mantle origin. Journal of Petrology, 32(1): 201

Sun SS and McDonough WF. 1989. Chemical and isotopic systematics of oceanic basalts: Implications for mantle composition and processes. In: Saunders AD and Norry MJ (eds.). Magmatism in Oceanic Basins. Geological Society London Special Publications, 42(1): 313 – 345

Tatsumi Y and Ishizaka K. 1981. Existence of andesitic primary magma: An example from southwest Japan. Earth and Planetary Science Letters, 53(1): 124 – 130

Tatsumi Y and Ishizaka K. 1982. Origin of high-magnesian andesites in the Setouchi volcanic belt, southwest Japan, I. Petrographical and chemical characteristics. Earth and Planetary Science Letters, 60(2): 293 – 304

Tatsumi Y and Maruyama S. 1989. Boninites and high-Mg andesites: Tectonics and petrogenesis. In: Crawford A (ed.). Boninites and Related Rocks. Unwin Hyaman, 50 – 71

Tatsumi Y. 2001. Geochemical modeling of partial melting of subducting sediments and subsequent melt-mantle interaction: Generation of high-Mg andesites in the Setouchi volcanic belt, Southwest Japan. Geology, 29(4): 323 – 326

Tatsumi Y and Hanyu T. 2003. Geochemical modeling of dehydration and partial melting of subducting lithosphere: Toward a comprehensive understanding of high-Mg andesite formation in the Setouchi volcanic belt, SW Japan. Geochemistry Geophysics Geosystems, 4(9): doi: 10.1029/2003GC00053

Tatsumi Y. 2006. High-Mg andesites in the Setouchi volcanic belt, southwestern Japan: Analogy to Archean magmatism and continental crust formation? Annual Review of Earth and Planetary Sciences, 34: 467 – 499

Wang FT. 2006. The Palacegeographic and Geo-ecological Atlas of Xinjiang Uygur Autonomous Region. Beijing: SinoMaps Press, 1 – 226 (in Chinese with English abstract)

Wang Q, McDermott F, Xu JF, Bellon H and Zhu YT. 2005. Cenozoic K-rich adakitic volcanic rocks in the Hohxil area, northern Tibet: Lower-crustal melting in an intracontinental setting. Geology, 33(6): 465 – 468

Wang Q, Wyman DA, Xu JF, Jian P, Zhao ZH, Li CF, Xu W, Ma JL and He B. 2007a. Early Cretaceous adakitic granites in the northern Dabie Complex, central China: Implications for partial melting and delamination of thickened lower crust. Geochimica et Cosmochimica Acta, 71(10): 2609 – 2636

Wang Q, Wyman DA, Zhao ZH, Xu JF, Bai ZH, Xiong XL, Dai TM, Li CF and Chu ZY. 2007b. Petrogenesis of Carboniferous adakites and Nb-enriched arc basalts in the Alataw area, northern Tianshan Range (western China): Implications for Phanerozoic crustal growth in the Central Asia orogenic belt. Chemical Geology, 236(1 – 2): 42 – 64

Wang Q, Xu JF, Jian P, Bao ZW, Zhao ZH, Li CF, Xiong XL and Ma JL. 2006a. Petrogenesis of adakitic porphyries in an extensional tectonic setting, dexing, South China: Implications for the genesis of porphyry copper mineralization. Journal of Petrology, 47(1): 119 – 144

Wang Q, Zhao ZH, Xu JF, Wyman DA, Xiong XL, Zi F and Bai ZH. 2006b. Carboniferous adakite-high-Mg andesite-Nb-enriched basaltic rock suites in the Northern Tianshan area: Implications for Phanerozoic crustal growth in the Central Asia Orogenic Belt and Cu-Au mineralization. Acta Petrologica Sinica, 22(1): 11 – 30(in Chinese with English abstract)

Wilson M. 1989. Igneous Petrogenesis. Springer, 1 – 466

Windley BF, Allen MB, Zhang C, Zhao ZY and Wang GR. 1990. Paleozoic accretion and Cenozoic redeformation of the Chinese Tien Shan Range, Central Asia. Geology, 18(2): 128 – 131

Xia LQ, Xia ZC, Xu XY, Li XM and Ma ZP. 2008. Relative contributions of crust and mantle to the generation of the Tianshan Carboniferous rift-related basic lavas, northwestern China. Journal of Asian Earth Sciences, 31(4 – 6): 357 – 378

Xia LQ, Xia ZC, Xu XY, Li XM, Ma ZP and Wang LS. 2004a. Carboniferous Tianshan igneous megaprovince and mantle plume. Geologcal Bulletin of China, 23(9): 903 – 910(in Chinese with English abstract)

Xia LQ, Xu XY, Xia ZC, Li XM, Ma ZP and Wang LS. 2004b. Petrogenesis of Carboniferous rift-related volcanic rocks in the Tianshan, northwestern China. Geological Society of America Bulletin, 116(3 – 4): 419 – 433

Xiao L and Clemens JD. 2007. Origin of potassic (C-type) adakite magmas: Experimental and field constraints. Lithos, 95(3 – 4):

399 – 414
Xiao WJ, Windley BF, Badarch G, Sun S, Li J, Qin K and Wang Z. 2004. Palaeozoic accretionary and convergent tectonics of the southern Altaids: Implications for the growth of Central Asia. Journal of the Geological Society, 161(3): 339 – 342
Xiao WJ, Han CM, Yuan C, Sun M, Lin SF, Chen HL, Li ZL, Li JL and Sun S. 2008. Middle Cambrian to Permian subduction-related accretionary orogenesis of Northern Xinjiang, NW China: Implications for the tectonic evolution of central Asia. Journal of Asian Earth Sciences, 32(2 – 4): 102 – 117
Xiong XL, Cai ZY, Niu HC, Chen YB, Wang Q, Zhao ZH and Wu JH. 2005. The Late Paleozoic adakites in eastern Tianshan area and their metallogenetic significance. Acta Petrologica Sinica, 21(3): 967 – 976 (in Chinese with English abstract)
Xu JF, Shinjo R, Defant MJ, Wang QA and Rapp RP. 2002. Origin of Mesozoic adakitic intrusive rocks in the Ningzhen area of east China: Partial melting of delaminated lower continental crust? Geology, 30(12): 1111 – 1114
Yuan HL, Gao S, Liu XM, Li HM, Gunther D and Wu FY. 2004. Accurate U-Pb age and trace element determinations of zircon by laser ablation-inductively coupled plasma mass spectrometry. Geoanalytical and Geostandard Newsletters, 28(3): 353 – 370
Zhai W, Sun XM, Gao J, He XP, Liang JL, Miao LC and Wu YL. 2006. SHRIMP dating of zircons from volcanic host rocks of Dahalajunshan Formation in Axi gold deposit, Xinjiang, China, and its geological implications. Acta Petrologica Sinica, 22(5): 1399 – 1404 (in Chinese with English abstract)
Zhang HF, Zhang L, Harris N, Jin LL and Yuan HL. 2006a. U-Pb zircon ages, geochemical and isotopic compositions of granitoids in Songpan-Garze fold belt, eastern Tibetan Plateau: Constraints on petrogenesis and tectonic evolution of the basement. Contributions to Mineralogy and Petrology, 152(1): 75 – 88
Zhang L, Shen Y and Ji J. 2003. Characteristics and genesis of Kanggur gold deposit in the eastern Tianshan mountains, NW China: Evidence from geology, isotope distribution and chronology. Ore Geology Reviews, 23(1 – 2): 71 – 90
Zhang LC, Qin KZ and Xiao WJ. 2008. Multiple mineralization events in the eastern Tianshan district, NW China: Isotopic geochronology and geological significance. Journal of Asian Earth Sciences, 32(2 – 4): 236 – 246
Zhang LC, Xiao WJ, Qin KZ, Ji JS and Yang XK. 2004. Types, geological features and geodynamic significances of gold-copper deposits in the Kanggurtag metallogenic belt, eastern Tianshan, NW China. International Journal of Earth Sciences, 93(2): 224 – 240
Zhang LC, Xiao WJ, Qin KZ and Zhang Q. 2006b. The adakite connection of the Tuwu-Yandong copper porphyry belt, eastern Tianshan, NW China: Trace element and Sr-Nd-Pb isotope geochemistry. Mineralium Deposita, 41(2): 188 – 200
Zhang Q, Qian Q and Wang EQ. 2001. An east China plateau in Mid-Late Yanshanian period: Implication from adakites. Chinese Journal of Geology, 36(2): 248 – 255 (in Chinese with English abstract)
Zhao ZH, Xiong XL, Wang Q, Wyman DA, Bao ZW, Bai ZH and Qiao YL. 2008. Underplating-related adakites in Xinjiang Tianshan, China. Lithos, 102(1 – 2): 374 – 391
Zhu YF, Zhang LF, Gu LB, Guo X and Zhou JB. 2005. The zircon SHRIMP chronology and trace element geochemistry of the Carboniferous volcanic rocks in western Tianshan Mountains. Chinese Science Bulletin, 50(19): 2201 – 2212
Zhu YF, Zhou JB and Guo X. 2006a. Petrology and Sr-Nd isotopic geochemistry of the Carboniferous volcanic rocks in the western Tianshan Mountains, NW China. Acta Petrologica Sinica, 22(5): 1341 – 1350 (in Chinese with English abstract)
Zhu YF, Zhou J, Song B *et al*. 2006b. Age of the "Dahalajunshan" Formation in Xinjiang and its disintegration. Geology in China, 33(3): 487 – 497 (in Chinese with English abstract)
Zhu ZX, Wang KZ, Xu D, Su YL and Wu YM. 2006. SHRIMP U-Pb dating of zircons from Carboniferous intrusive rocks on the active continental margin of Eren Habirga, West Tianshan, Xinjiang, China, and its geological implications. Geological Bulletin of China, 25(8): 986 – 991 (in Chinese with English abstract)

## 附中文参考文献

车自成,刘良. 1996. 论伊犁古裂谷. 岩石学报, 12(3): 478 – 490
贾斌,毋瑞身,田昌烈,沙德铭,杨森. 2001. 塔吾尔别克一阿庇因迪斑岩型金矿特征. 地质与资源, 10(3): 139 – 145
李华芹. 1998. 新疆北部有色贵金属矿床成矿作用年代学. 北京: 地质出版社
李华芹, 王登红, 万阈, 屈文俊, 张兵, 路远发, 梅玉萍, 邹绍利. 2006. 新疆莱历斯高尔铜钼矿床的同位素年代学研究. 岩石学报, 22(10): 2437 – 2443
李锦轶, 王克卓, 孙桂华, 莫申国, 李文铅, 杨天南,高立明. 2006. 东天山吐哈盆地南缘古生代活动陆缘残片:中亚地区古亚洲洋板块俯冲的地质记录. 岩石学报, 22(5): 1087 – 1102
龙灵利, 高俊, 钱青, 熊贤明, 王京彬, 王玉往, 高立明. 2008. 西天山伊犁地区石炭纪火山岩地球化学特征及构造环境. 岩石学报, 24(4): 699 – 710
沙德铭, 金成洙, 董连慧, 毋瑞身, 田昌烈,贾斌. 2005. 西天山阿希金矿成矿地球化学特征研究. 地质与资源, 14(2): 118 – 125
王福同. 2006. 新疆维吾尔自治区古地理及地质生态图集. 北京: 中国地图出版社
王强, 赵振华, 许继峰, Wyman DA, 熊小林, 资峰,白正华. 2006. 天山北部石炭纪埃达克岩-高镁安山岩-富 Nb 岛弧玄武质岩:对中亚造山带显生宙地壳增生与铜金成矿的意义. 岩石学报, 22(1): 11 – 30
夏林圻, 夏祖春, 徐学义, 李向民, 马中平,王立社. 2004. 天山石炭纪大火成岩省与地幔柱. 地质通报(9): 903 – 910
熊小林, 蔡志勇, 牛贺才, 陈义兵, 王强, 赵振华, 吴金花. 2005. 东天山晚古生代埃达克岩成因及铜金成矿意义. 岩石学报, 21(3): 967 – 976
翟伟, 孙晓明, 高俊, 贺小平, 梁金龙, 苗来成, 吴有良. 2006. 新疆阿希金矿床赋矿围岩-大哈拉军山组火山岩 SHRIMP 锆石年龄及其地质意义. 岩石学报, 22(5): 1399 – 1404
张旗, 钱青,王二七. 2001. 燕山中晚期的中国东部高原:埃达克岩的启示. 地质科学, 36(2): 248 – 255
朱永峰, 周晶,郭璇. 2006a. 西天山石炭纪火山岩岩石学及 Sr-Nd 同位素地球化学研究. 岩石学报, 22(5): 1341 – 1350
朱永峰, 周晶, 宋彪等. 2006b. 新疆"大哈拉军山组"火山岩的形成时代问题及其解体方案. 中国地质, 33(3): 487 – 497
朱志新, 王克卓, 徐达, 苏延龙,吴玉门. 2006. 依连哈比尔尕山石炭纪侵入岩锆石 SHRIMP U-Pb 测年及其地质意义. 地质通报, 25(8): 986 – 991